CHANGES IN CHLOROPHYLL-A CONCENTRATION AS AN INDICATOR OF PRIMARY PRODUCTIVITY IN WATERS BEFORE AND AFTER SEA FENCING ON THE COAST OF TANGERANG, INDONESIA

Najwa ELZAHRA [1], Luthfi ANZANI [1], Yulius YULIUS [2*], Muhammad RAMDHAN [3], Dini PURBANI [2], Aprizon PUTRA [2], Taslim ARIFIN [2], Hadiwijaya L. SALIM [2], Anang D. PURWANTO [2], Joko PRIHANTONO [2], Rinny RAHMANIA[2], Sri Endah PURNAMANINGTYAS [2], Herlina Ika RATNAWATI [2]

DOI: 10.21163/GT_2026.211.01

ABSTRACT

Coastal eutrophication is an escalating concern in Indonesian estuaries, driven by anthropogenic pressures and physical interventions such as sea fencing. This study analyses the spatial and temporal changes in Chlorophyll-a (Chl-a) concentrations and Net Primary Productivity (NPP) in the coastal waters of Kronjo, Tangerang Regency, before (2020) and after (2024) the installation of illegal sea fences. High-resolution (3 m) PlanetScope satellite imagery was processed using the Normalised Difference Chlorophyll Index (NDCI) and subsequently modelled into NPP using the Vertically Generalised Productivity Model (VGPM), incorporating supporting data such as Photosynthetically Active Radiation (PAR), Sea Surface Temperature (SST), and Euphotic Zone Depth (Zeu). Despite an increase in localised maximum values, the results revealed a slight decrease in mean Chl-a concentrations from 6.12 to 5.89 mg/m^3. The spatial distribution of NPP became more homogenised, with high-value areas becoming more spatially constrained. A robust Pearson correlation ($r = 0.99$; $p < 0.001$) between Chl-a and NPP confirms the reliability of NDCI for capturing primary productivity dynamics. This study demonstrates the efficacy of high-resolution remote sensing in evaluating the ecological impacts of coastal physical structures and informing spatially explicit management strategies. This is the first high-resolution remote sensing study assessing Southeast Asia's pre- and post-se fencing impacts, highlighting the critical need for integrated spatial monitoring in tropical estuarine ecosystems.

Key-words: *Chlorophyll-a; Estuarine monitoring; PlanetScope; Primary productivity; Sea fence.*

1. INTRODUCTION

Indonesia is an archipelagic country with a maritime area of over 6.4 million km² and a coastline of approximately 108,000 km (Yanuar et al., 2023). Its coastal regions are central to a country's development and ecological resilience. Approximately 22% of Indonesia's population resides in coastal regions and relies on fishing, trade, tourism, and maritime transport activities for livelihoods (Jamal, 2019). These activities make the coast a national economic hub and increase pressure on the coastal environment.

---

[1]*Indonesia University of Education (UPI), Bandung-West Java, Indonesia. (NE) najwaelzr26@upi.edu; (LA) luthfi_anzani@upi.edu*
[2]*National Research and Innovation Agency (BRIN), Bogor-West Java, Indonesia. (YY) yuli058@brin.go.id; (DP) dini017@brin.go.id, (AP) apri024@brin.go.id; (TA) tasl003@brin.go.id; (HLS) hadi026@brin.go.id; (ADP) anan009@brin.go.id; (JP) joko.prihantono@brin.go.id; (RR) rinny.rahmania@brin.go.id; (SEP) srie005@brin.go.id; (HIR) herl010@brin.go.id*
[3]*National Research and Innovation Agency (BRIN), Bandung-West Java, Indonesia. (MR) muha307@brin.go.id*
[*]*Corresponding author email: yuli058@brin.go.id*

One coastal region that reflects the complexity of interactions between oceanographic processes and anthropogenic pressures is the Kronjo estuary on the northern coast of Tangerang Regency, Banten Province, Indonesia. This area is influenced by the flow of the Cidurian River and its tributaries (Kali Malang-Muara Selasih and Cipasilian), as well as by micro-tidal dynamics and land runoff (Laksana, 2011; Fadlillah et al., 2018).

In recent decades, this area has experienced significant water quality degradation due to domestic industrial waste, reclamation, and infrastructure development, triggering local eutrophication (Wijayanti et al., 2022). The main parameters for evaluating the quality of aquatic ecosystems are Chlorophyll-a (Chl-a) concentration and Net Primary Productivity (NPP) (Fan et al., 2023). Chl-a is the primary photosynthetic pigment in phytoplankton, which is highly sensitive to light, nutrients, and water turbidity variations. In the tropical coastal waters of Indonesia, Chl-a has been shown to have a robust correlation with marine primary productivity, with a coefficient of determination $R^2 \geq 0.9$ (Arridhaty Akita et al., 2023; Nuzapril et al., 2019). Local studies in the Karimun Jawa Islands, Lake Lait, and Tangkil Island support these findings, with R^2 values up to 0.99 (Nuzapril et al., 2017; Fitra et al., 2013; Fathia et al., 2021).

The latest physical stress has emerged on the coast of Tangerang Regency since 2021, namely massive unauthorised sea fencing constructed using bamboo. These structures can modify tidal currents, trap sediments, and reduce water transparency, suppressing phytoplankton biomass and primary productivity. A similar phenomenon has been reported in Jinmeng Bay, China, where a land reclamation project involving the creation of artificial islands has led to a 35% increase in water residence time, a decrease in nutrient diffusion capacity, and an increased risk of eutrophication and algal blooms (Kuang et al., 2024). Studies in the Malacca Strait also showed a decrease in Chl-a concentrations from 7-9 mg/L to 5-7 mg/L after reclamation, with a significant correlation to changes in Total Suspended Solids (TSS), Sea Surface Temperature (SST), and tidal currents (Abdullah & Dusuki, 2018). Additionally, the spatial-temporal distribution of Chl-a in the Pearl River Estuary is significantly influenced by anthropogenic activities and changes in water dynamics (Fan et al., 2023).

Through the Ministry of Marine Affairs and Fisheries or KKP (2025), the Indonesian government has also stated that sea fencing can seriously threaten the balance of marine ecosystems. However, there are no high-resolution quantitative spatial-temporal studies explicitly comparing ecosystem conditions before and after the installation of coastal physical structures such as sea fences in Indonesia. Direct monitoring in shallow and muddy waters, such as Kronjo, often faces access and cost limitations. Therefore, remote sensing can effectively and efficiently monitor spatial-temporal changes (Yulius et al., 2021). Satellite imagery such as the Moderate Resolution Imaging Spectroradiometer (MODIS) or Sentinel-2 has been widely used, but its low resolution makes it unsuitable for monitoring local changes on a metre scale. PlanetScope, satellite imagery with a spatial resolution of 3 metres and daily recording frequency, can detect subtle spatial dynamics in narrow areas such as Kronjo. The Normalised Difference Chlorophyll Index (NDCI) algorithm, which utilises the red (665 nm) and red-edge (708 nm) bands, has proven accurate for estimating Chl-a in turbid and shallow waters (Mishra & Mishra, 2012). In a study by Wasehun et al. (2025), PlanetScope was superior in capturing fine spatial dynamics in small water bodies and producing relatively high Chl-a estimation accuracy values ($R^2 = 0.71$). This supports the use of PlanetScope imagery in studies of narrow areas such as Kronjo Sub-district.

To support a more comprehensive assessment of ecosystem productivity, NDCI can be integrated with parameters such as Photosynthetically Active Radiation (PAR) and SST in the Vertically Generalised Productivity Model (VGPM) to obtain NPP values (Behrenfeld & Falkowski, 1997). Similar studies in tropical regions show that NPP and Chl-a follow the same seasonal patterns and are strongly influenced by environmental variability, including The El Niño-Southern Oscillation (ENSO) effects, seasonal changes, and human interventions (Dewi et al., 2018; Marpaung et al., 2022; Nugraheni et al., 2014). This study aims to analyse the spatial and temporal changes in Chl-a and NPP concentrations in Kronjo waters before (2020) and after (2024) the installation of sea fences. In addition, this study will evaluate the impact of sea fencing on Chl-a dynamics by combining the NDCI algorithm and the VGPM model based on PlanetScope imagery. This study is expected to fill the gap

in study on the physical effects of sea fences on tropical waters and offer a spatially detailed approach that can be used to support coastal management policies and serve as a reference for similar studies in Southeast Asia.

2. STUDY AREA

Kronjo Sub-district is one of the coastal regions in Tangerang Regency, Banten Province, Indonesia, located on the northern coast of Java Island and directly bordering the Java Sea. Geographically, Kronjo Sub-district is located at approximately 6° 03′37″ South Latitude and 106° 25′27″ East Longitude and has a relatively long coastline with waters dominated by river estuaries and estuary areas. This area is a transitional zone between fluvial and marine systems, influenced by micro-tidal fluctuations, dominant west-to-east coastal currents, and nutrient inputs from the mainland, particularly from the Cidurian, Cipasilian, and Cimanceuri rivers. Its coastal geomorphological characteristics include swampy land, ponds, and secondary mangrove vegetation, making the region highly sensitive to natural and anthropogenic environmental changes. Starting in 2021, physical intervention in sea fence construction using bamboo structures and nets has occurred at several coastal locations in Kronjo. These structures were built without hydrodynamic studies or official permits and have been reported to harm the coastal ecosystem. A spatial overview of the study location is shown in **figure 1**, which shows the river flow system and the location of the sea fences on the coast of Kronjo Kronjo Sub-district.

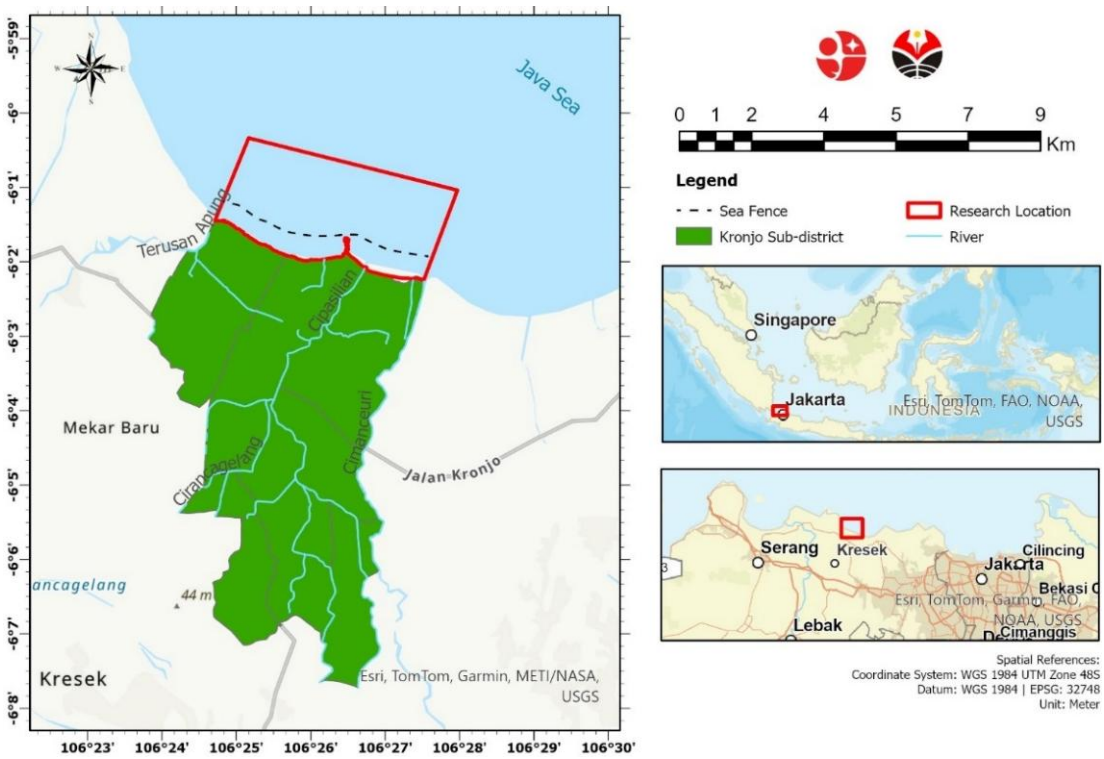

Fig. 1. Map of the study area.

3. DATA AND METHODS

This study method began with problem identification, followed by data collection that included PlanetScope satellite imagery, PAR, and SST. PlanetScope imagery was processed to calculate the Normalised Difference Water Index (NDWI) to separate water areas, which were then used in NDCI

calculations and Chl-a estimates. The Chl-a, PAR, and SST parameters are then entered into the VGPM to calculate NPP. The estimated NPP and Chl-a results are analysed using Pearson's correlation to evaluate the relationship between variables. The final stage of the study is interpreting the correlation results and spatial distribution to understand the dynamics of primary productivity changes in the study area. The study workflow is shown in **figure 2** below.

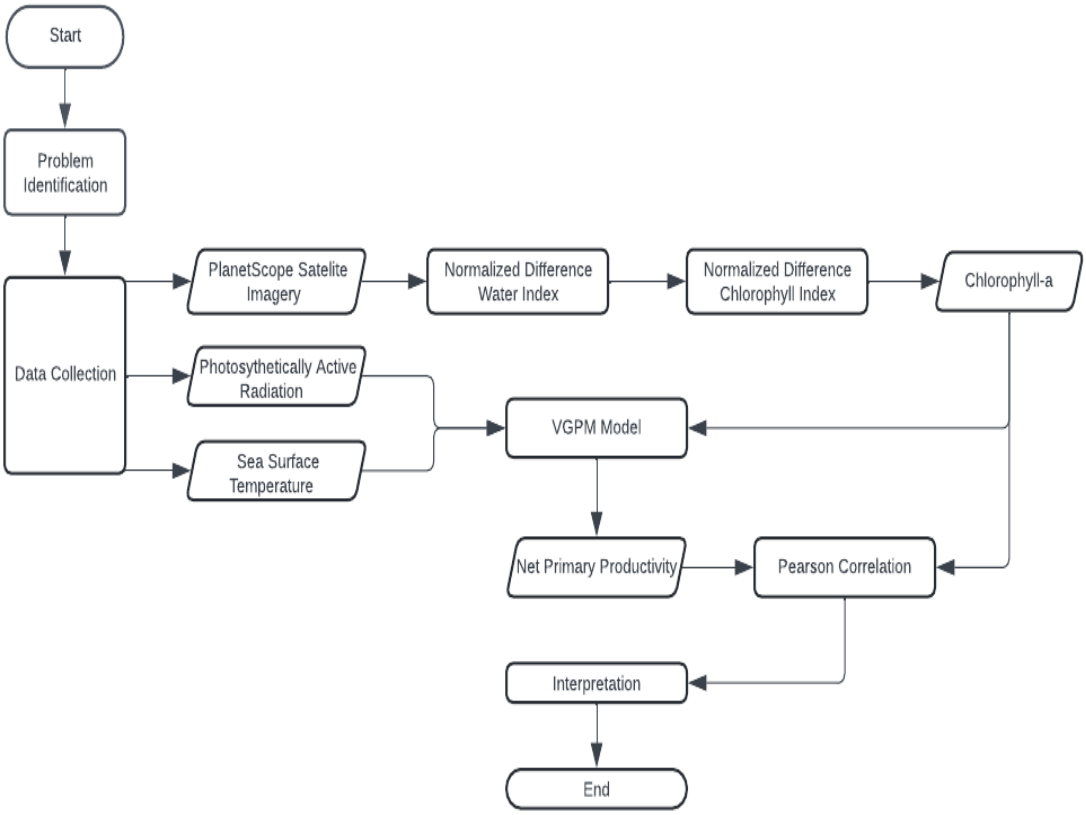

Fig. 2. Flowchart.

3.1. Data

This study utilises PlanetScope satellite imagery of the Analytic MS_SR 8-band type, which has undergone atmospheric correction (Surface Reflectance). The imagery has a spatial resolution of 3 m, with additional information including sun elevation angle, off-nadir angle, and cloud cover percentage. The dataset used covers two observation periods June 20, 2020 (pre-fencing) and October 26, 2024 (post-fencing), with a cloud cover criterion of <10%. Each image covers eight spectral channels, with the bands used in the analysis having the following criteria. More details can be seen in **table 1** below.

Table 1.

PlanetScope spectral channels and their use in analysis.

Band	Spectral Name	Wavelength (nm)	Function
B4	Green	~550	NDWI, Zeu
B6	Red	~665	NDCI
B7	Red edge	~705	NDCI
B8	Near Infrared (NIR)	~865	NDCI, Shadow

Source : https://developers.planet.com/docs/apis/data/sensors/

The following supporting data was used (in **table 2**).

Table 2.

Supporting data for NPP.

Parameters	Data Source	Spatial Resolution	Temporal Resolution
PAR	MODIS-Aqua L3 PAR	4 km	Daily
SST	MODIS-Aqua L3 SST	4 km	Daily
Precipitation	CHIRPS v2.1	0.05° (~5 km)	Daily

3.2. Methods

This study uses a quantitative approach based on remote sensing to identify and compare spatial and temporal changes in water physical-chemical parameters, particularly Chl-a and NPP, before and after the installation of marine fencing on the Kronjo coast, Tangerang Regency. The analysis was carried out through the following series of processes.

3.2.1. Pre-processing and Masking

The image used is PlanetScope AnalyticMS_SR, which is at the Surface Reflectance (SR) level, so no additional atmospheric correction is required. Before calculating the index, cloud, shadow, and water masking is performed to ensure that only undisturbed water areas are analysed.

- Cloud Masking: Clouds generally have very high reflectance in the visible channel, especially in the green and red channels. Based on the harmonised PlanetScope SR usage documentation for analysis purposes. The 2500 DN threshold corresponds to a reflectance of approximately 0.25 (on a scale of 0–10,000), indicating thick clouds with high reflectance. This threshold minimises the misclassification of very bright pixels as clouds, the following empirical thresholds are used.

$$Green > 2500 \text{ and } Red > 2500$$

- Shadows (from both clouds and topographic surfaces) exhibit very low reflectance values in the visible and NIR channels. The 500 Digital Number (DN) threshold on a 0–10,000 scale corresponds to a reflectance value of approximately 0.05, which aligns with the characteristics of dark areas. This technique is commonly used in shadow masking algorithms for high-resolution imagery such as Landsat/Sentinel (e.g., Fmask) and has been adapted for PlanetScope SR. Following the cloud and shadow masking procedures, only water pixels that were completely free from contamination were retained. As a result, the final region of interest (ROI) selected for the Chl-a and NPP analysis consisted entirely of clear-sky and non-shadowed areas. Therefore, 100% of the analysed area was classified as valid, ensuring high spatial integrity and reliability in the results. Therefore, pixels are classified as part of a shadow if.

$$Green > 500 \text{ and } NIR > 500$$

- Water Masking: The masking of water areas was carried out using the Normalised Difference Water Index (NDWI) (McFeeters, 1996), which is a remote sensing technique developed by McFeeters (1996) to detect and separate water features from land and terrestrial vegetation. This index is handy in identifying water bodies in satellite images because it utilises the difference in reflectance characteristics between the green and near-infrared (NIR) channels. Water typically has low reflectance to NIR light and high reflectance to green light, while vegetation and dry soil show the opposite pattern. NDWI values greater than zero (NDWI > 0) are interpreted as water bodies, and these pixels are then used for NDCI-based Chl-a index calculations. The NDWI equation used refers to the formula from McFeeters (1996).

$$NDWI = \frac{Green - NIR}{Green + NIR}$$

where: Green = Band 4; and NIR = Band 8.

3.2.2. Indeks NDCI

NDCI has been recognised as one of the most efficient and practical methods for estimating Chl-a concentrations in various water bodies. Numerous studies have documented its practical application in Case II waters (An Ru et al., 2013), coastal estuaries (Mishra et al., 2014), and bay areas (Manuel & Blanco, 2023). Compared to other methods, NDCI offers ease of application, estimation accuracy, and flexibility in cross-platform remote sensing use (An Ru et al., 2013). Furthermore, several studies have shown a strong correlation between NDCI values and in situ measured Chl-a concentrations, with reported determination coefficients (R^2) ranging from 0.74 to 0.96 (Mishra et al., 2014; Manuel & Blanco, 2023). This indicates the consistency of NDCI in describing the spatial and temporal variability of primary productivity in water bodies. NDCI is calculated based on the formulation introduced by Mishra & Mishra (2012) as follows.

$$NDCI = \frac{R_{red-edge} - R_{red}}{R_{red-edge} + R_{red}}$$

where: $R_{red-edge}$ = Band 7; and R_{red} = Band 6.

The NDCI values obtained were then converted to Chl-a (mg/m³) using the equation from the Mishra & Mishra (2012) study, which is widely applied in tropical regions:

$$Chl\text{-}a = a \times e^{b.NDCI}$$

where: NDCI = Calculated from the Red Edge (708 nm) and Red (665 nm) channels; Chl- a = Chl-a concentration (mg/m³); a = Scale constant (intercept) from regression results; b = Slope coefficient from regression results; and e = Euler's number, the basis of natural logarithms.

This model is widely used in tropical regions because it has been tested under high nutrient and light fluctuations and turbidity conditions. This algorithm was applied to high-resolution imagery in the study by Saulquin et al. (2019). It showed spatial consistency with in situ data, making it ideal for monitoring coastal waters in developing regions. The following **table 3** shown the classification of Chl-a concentrations based on NDCI values for ecological interpretation.

Table 3.

Classification of Chl-a values based on the NDCI index.

NDCI Range	Chl-a Range (mg/m³)
< -0	< 7.5
-0.1 to 0	7.5 - 16
0 to 0.1	16 - 25
0.1 to 0.2	25 - 33
0.2 to 0.4	33 - 50
0.4 to 0.5	> 50
0.5 to 1	Severe bloom

Source: Mishra & Mishra (2012).

The application of NDCI in this study enabled the identification of productive and eutrophic zones and the detection of possible ecological disturbances caused by human interventions such as marine fencing. The strong correlation between NDCI and Chl-a, which has been proven in various studies, makes this method valid for assessing changes in water quality spatially and temporally.

3.2.3. NPP

NPP can be estimated using the VGPM global scale model with remote sensing satellite image data inputs (Behrenfeld & Falkowski, 1997; Marpaung et al., 2022). This model calculates NPP (in units of mg C/m²/day) based on Chl-a concentration, PAR, Zeu, and maximum daily phytoplankton productivity P_b^{opt}, which is controlled by SST, using the following equation.

$$NPP = 0.66125 \times P_b^{opt} \times \left(\frac{E_{PAR}}{E_{PAR} + 4.1}\right) \times C_{sat} \times Z_{eu}$$

where: P_b^{opt} = Optimal productivity parameters, depending on temperature; C_{sat} = Chl-a concentration (mg/m³); E_{PAR} = Photosynthetic active radiation intensity (Einstein/m²/day); Z_{eu} = Depth of the Euphotic zone (m).

3.2.4. Pearson Correlation

To assess the relationship between Chl-a concentration and NPP, Pearson's correlation analysis (r) was performed, assuming a normal distribution and a linear relationship between variables. The analysis was conducted on paired samples for 2020 and 2024, using data from raster to sampling points obtained from the NDWI masking process. The correlation was considered strong if $r > 0.8$, and statistical significance was determined with $p < 0.05$. This analysis refers to the classical statistical method by Pearson (1896), which has been revisited and widely used in modern oceanography and ecology study (Marpaung et al., 2022). Pearson's correlation (r) was calculated using the formula.

$$r = \frac{r\sum xy - \sum x \sum y}{\sqrt{[n\sum x^2 - (\sum x)^2][n\sum y^2 - (\sum y)^2]}}$$

where: x = Chl-a (mg/m³); y = NPP mg C/m²/day; and n = Sample size.

Pearson's correlation is used to evaluate the extent to which two variables are related. A Pearson correlation value (r) close to +1 or -1 indicates a robust linear relationship with a positive or negative direction. If the r value is positive ($r > 0$), then the relationship between the variables is unidirectional, and the higher the value, the stronger the relationship. Conversely, $r < 0$ indicates an inverse relationship but is still strong. If the r value approaches zero, the relationship between the variables is considered weak or statistically insignificant (Walpole, 2012; Sambah et al., 2020). Generally, an r value > 0.8 is categorised as a strong correlation, with a significance level accepted if $p < 0.05$. This approach follows Pearson (1896), which is still widely applied in spatial relationship analysis in modern oceanography and ecology.

4. RESULTS

4.1. Spatial changes in NDCI

The spatial distribution of NDCI values as a bio-optical indicator of Chl-a shows striking spatial-temporal variations between the two observation periods. In 2020 (pre-fencing), the maximum NDCI value was 0.245, with a fairly widespread distribution of positive values in the eastern and central coastal regions. This indicates a high abundance of phytoplankton, particularly in the nutrient-rich estuary of the Cidurian River, which receives significant terrestrial runoff. Conversely, in 2024 (post-fencing), the maximum NDCI value was 0.428, but areas with negative NDCI values (< 0) expanded significantly, particularly in regions bounded by the sea fence. The distribution map of NDCI values can be seen in **figure 3** below. These findings indicate decreased primary productivity homogeneity and local accumulation of Chl-a in enclosed areas due to nutrient circulation and distribution disruption. Activities around the coast, such as reclamation and especially the construction of sea fences, contribute to changes in the distribution and concentration of Chl-a in the water. The interpretation of the values occurring before and after the construction of the sea wall can be seen in **table 4** below and in **table 5,** the comparison of Chl-a before and after sea walling.

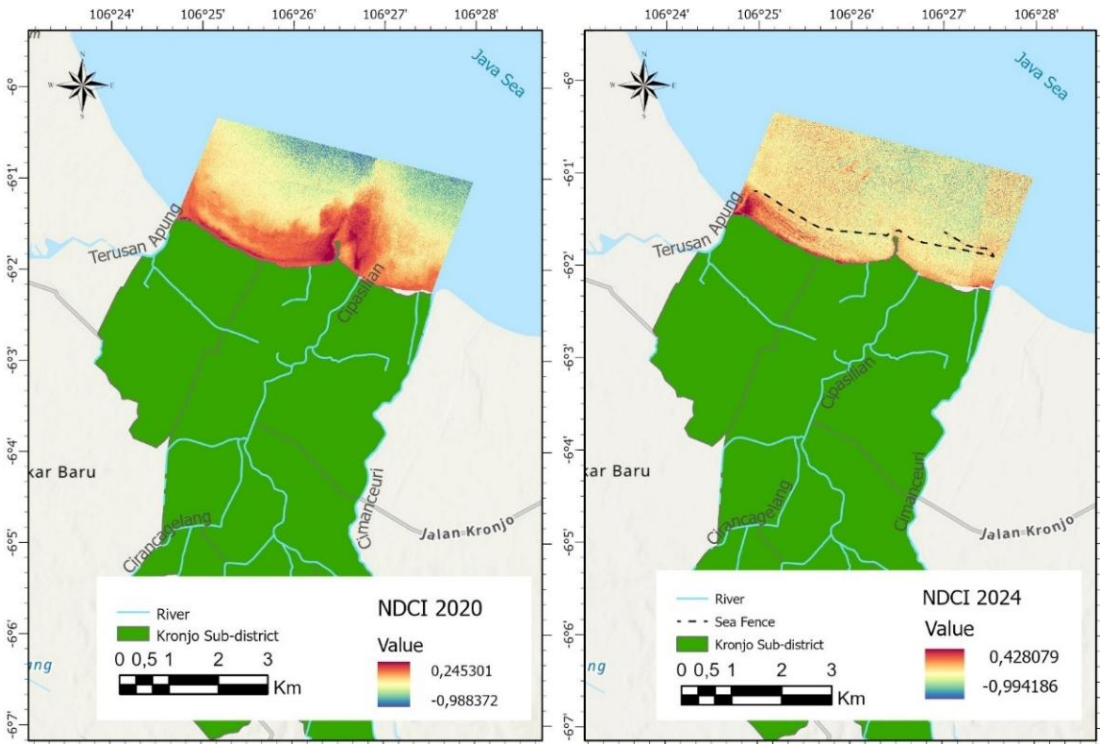

Fig. 3. Spatial distribution map of NDCI values in June 2020 (pre-fencing) and October 2024 (post-fencing).

Table 4.

Comparison of NDCI values before and after sea fencing.

Year	Min	Max	Mean	STD
2020	-0.988	0.245	-0.169	0.140
2024	-0.994	0.428	-0.155	0.086

Source: Data analysis, 2025.

4.2. Spatial changes in Chl-a

As the primary pigment for photosynthesis in phytoplankton, Chl-a reflects the dynamics of water fertility. In 2020, the maximum value was 30.16 mg/m³ with an average of 6.12 mg/m³. By 2024, the maximum value increased to 65.47 mg/m³, but the average decreased to 5.89 mg/m³. The distribution map of Chl-a can be seen in **figure 4** below.

Similar to what happened with NDCI values, the increase in maximum Chl-a values was not accompanied by an increase in the average area of this area, reflecting the presence of local eutrophication due to water stagnation. The area enclosed by the sea fence became a place accumulating nutrients and Chl-a, but overall productivity actually decreased. These findings support studies by Mishra & Mishra (2012); Manuel & Blanco (2023), which state that Chl-a is a sensitive indicator of physical disturbances and water dynamics.

Table 5.

Comparison of Chl-a before and after sea walling.

Year	Min	Max	Mean	STD
2020	0.16	30.16	6.12	3.40
2024	0.15	65.47	5.89	2.29

Source: Data analysis, 2025.

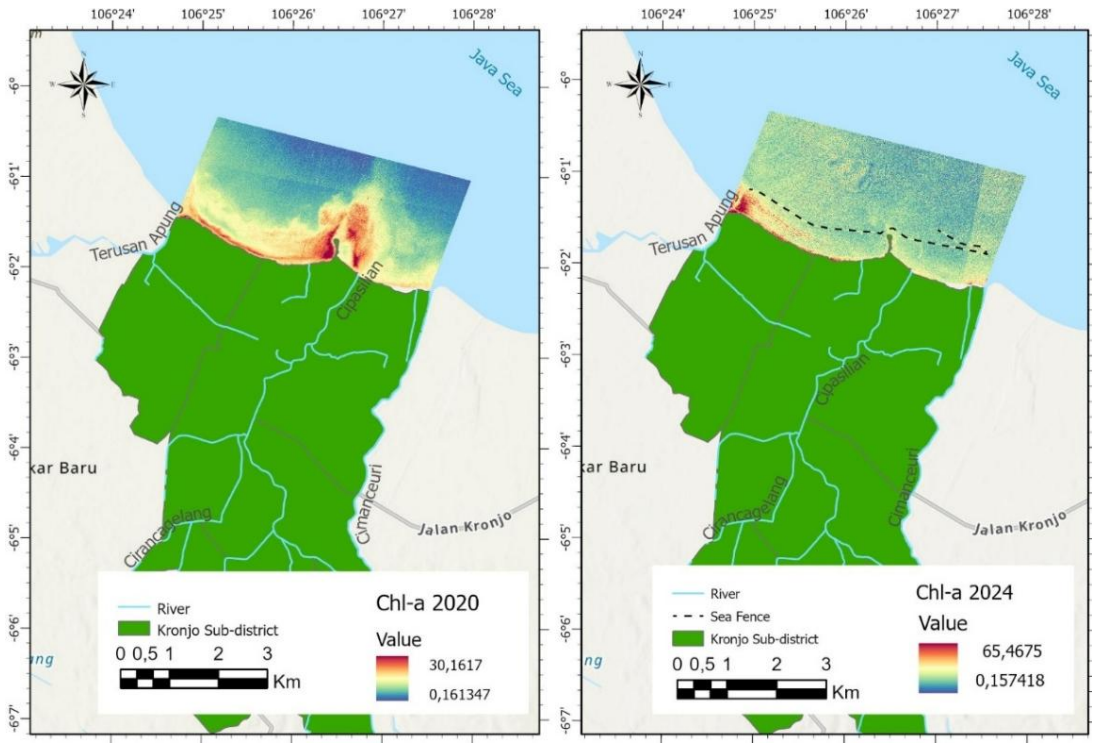

Fig. 4. Spatial distribution map of Chl-a in June 2020 (pre-fencing) and October 2024 (post-fencing).

4.3. Estimation and Distribution of NPP

NPP, estimated using the VGPM, which integrates Chl-a concentration, Euphotic Zeu, PAR, and SST, shows a spatial pattern consistent with the distribution of Chl-a. In 2020 (before the installation of the sea fence), NPP ranged from 3.23 to 64.82 mg C/m²/day, with an average of 26.91 mg C/m²/day. In 2024 (after the installation of the sea fence), the range increased to 3.17 to 96.63 mg C/m²/day, although the average decreased slightly to 26.80 mg C/m²/day. Maps of the spatial distribution of these values are shown in **figure 5** below.

As shown in **table 6**, although the average values appear relatively stable in both periods, the spatial distribution of NPP shows clear homogenisation. High-productivity zones have become increasingly fragmented and localised, reflecting the spatial patterns observed in the NDCI and Chl-a maps. This indicates that the presence of the sea fence has disrupted nutrient circulation and vertical mixing, causing primary productivity to concentrate in limited and stagnant zones. These findings align with previous studies highlighting the sensitivity of NPP to bio-optical and physical parameters of the water column.

Table 6.

Comparison of NPP before and after sea walling.

Year	Min	Max	Mean	STD
2020	3,23	64,82	26,91	5,31
2024	3,17	96,63	26,80	5,32

Source: Data analysis, 2025.

According to the trophic classifications proposed by Vollenweider (1968) and Rodhe (1969), as cited in Kumar et al. (2023), oligotrophic waters are defined as having daily NPP values of 65-300 mg C/m² and 30-100 mg C/m², respectively. With average values of less than 27 mg C/m²/day recorded in 2020 and 2024, the waters of Kronjo fall well below both thresholds, particularly even below Rodhe's lower limit.

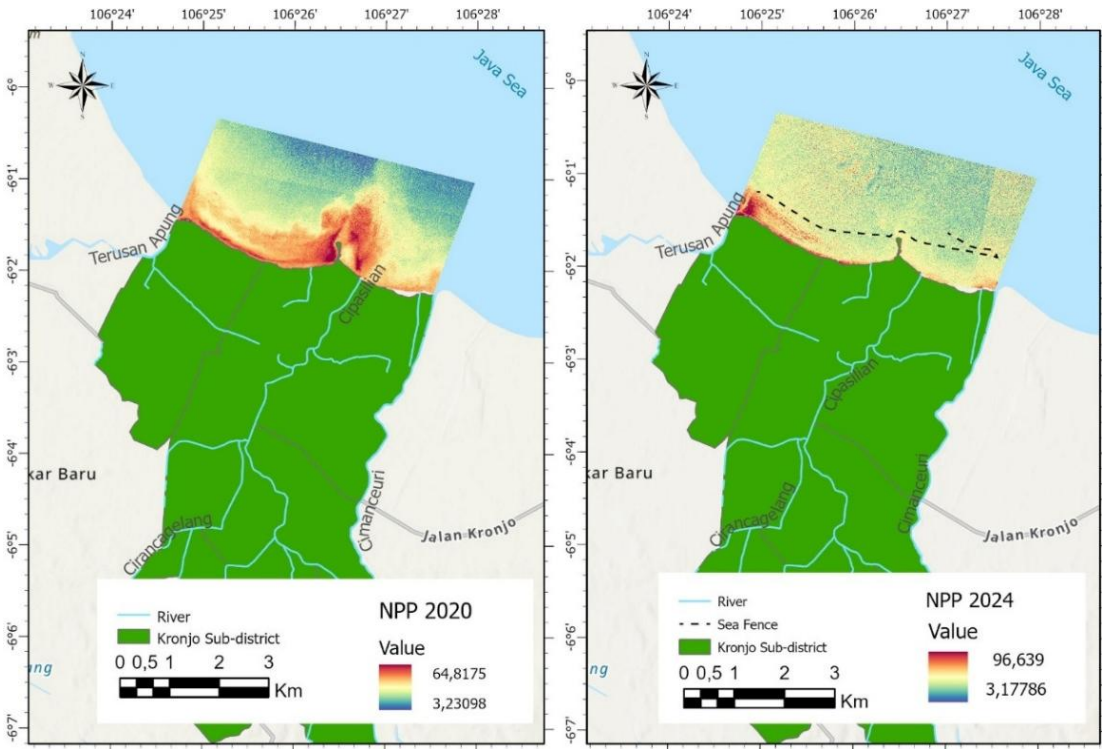

Fig. 5. Spatial distribution map of NPP in June 2020 (pre-fencing) and October 2024 (post-fencing).

This places the study area in a severely nutrient-deficient state, indicating a very low level of primary productivity. These results confirm that the Kronjo coastal waters are not only outside the productive range of typical oligotrophic systems but may represent an ultra-oligotrophic condition, which is ecologically concerning for a tropical coastal zone. The disruption in hydrodynamics caused by the sea fence, combined with limited land-based nutrient inputs, has likely constrained phytoplankton growth and reduced overall ecosystem function in the area.

4.4. The effect of rainfall on water dynamics

Precipitation is one of the main climatological factors affecting primary productivity in coastal regions, particularly through runoff mechanisms that carry nutrients from land to water. Based on CHIRPS (Climate Hazards Group InfraRed Precipitation with Station) data, monthly rainfall in the study area was recorded at 84.17 mm in June 2020 and 46.67 mm in October 2024 (**figure 6**). Although there was no rainfall on the main observation dates (20 June 2020 and 26 October 2024), the high monthly precipitation accumulation still significantly impacted water fertility dynamics.

During June 2020, relatively high rainfall likely contributed to increased runoff from the Cidurian River, its tributaries, and adjacent irrigation networks along the Kronjo coastline. This runoff may have introduced dissolved nutrients such as nitrogen and phosphate into the coastal waters, potentially supporting phytoplankton growth. According to Suardiani et al. (2018), rainfall in tropical coastal regions can increase phytoplankton biomass by supplying land-derived nutrients. In this period, the average Chl-a concentration reached 6.12 mg/m^3, accompanied by a uniform spatial distribution of NPP across the estuarine zone. Comparable responses to precipitation have been documented elsewhere. Prabuwono et al. (2023) observed that heightened runoff in the southern Red Sea was associated with increased Chl-a concentrations exceeding 1.3 mg/m^3, while Herdianti et al. (2023) emphasised the role of seasonal precipitation variability in modulating Chl-a and NPP in tropical shallow coastal systems.

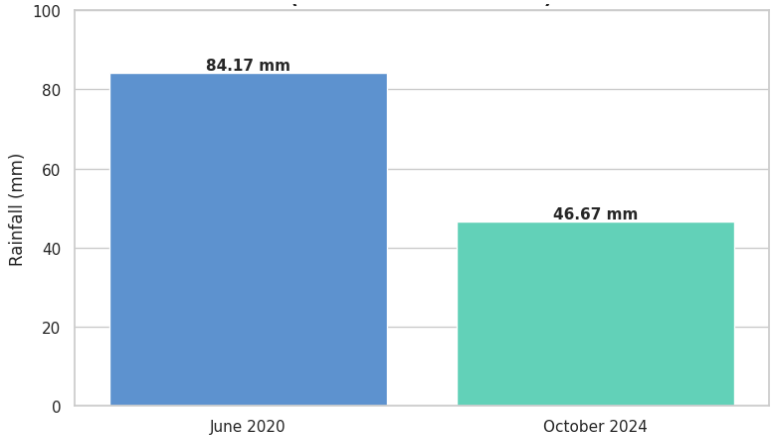

Fig. 6. Monthly rainfall graph in June 2020 and October 2024.

In contrast, October 2024 was characterised by a significant decline in monthly rainfall-nearly 50% lower than in June 2020, coinciding with a sea fence structure that physically restricted water circulation and vertical mixing. Although localised Chl-a maxima reached 65.47 mg/m^3, the overall average concentration declined to 5.89 mg/m^3, and NPP distribution became more spatially confined. These observations indicate the emergence of localised eutrophication, likely driven by the reduced exchange of nutrients in semi-enclosed areas.

Overall, the results suggest that the productive conditions observed in 2020 were shaped by a combination of hydrological and physical factors, including nutrient delivery and water circulation. In the case of Kronjo' s coastal waters, monthly rainfall should be considered a contributing driver of nutrient dynamics, particularly when interpreted alongside anthropogenic modifications and hydrodynamic constraints.

4.5. Relationship between Chl-a concentration and NPP

Pearson's correlation analysis between Chl-a concentration and NPP values showed a robust and statistically significant relationship in both years of observation. The correlation test results are shown in **figure 7** below.

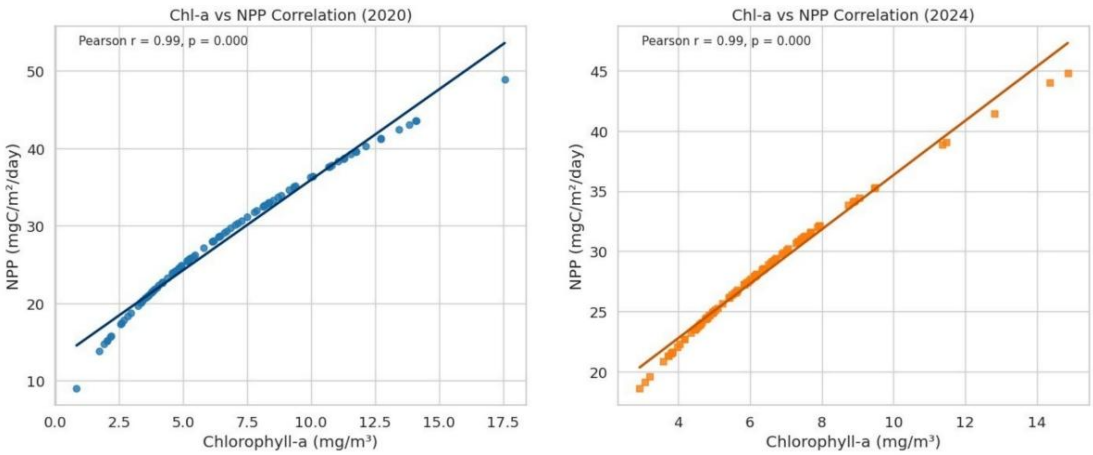

Fig. 7. The linear relationship between Chl-a and NPP in 2020 and 2024.

In 2020, the Pearson correlation between Chl-a and NPP reached r = 0.99 with a significance value of p = 0.000, indicating an almost perfect linear relationship. This reflects that variations in Chl-a concentration explain almost all variations in NPP values in conditions before marine fencing. Most data points show a consistent positive trend, indicating that increases in phytoplankton biomass directly enhance primary productivity in the water. In 2024, a similar relationship remained strong, with a value of r = 0.99 and p = 0.000. Although the correlation remained high, the distribution of points tended to be more concentrated in the Chl-a range of 5-10 mg/m³, with a few outliers at high values. This indicates that despite the implementation of marine fencing and changes in the spatial pattern of Chl-a, the functional relationship between phytoplankton biomass and productivity remains intact. However, the spatial homogenisation of NPP (discussed in Section 3.3) suggests that productivity contributions tend to be more locally concentrated post-fencing (not spatially extensive).

These findings reinforce previous study results that Chl-a is a strong indicator for estimating primary productivity in tropical coastal waters (Behrenfeld & Falkowski, 1997; Werdell et al., 2013). The strong correlation likewise reflects the reliability of the NDCI algorithm in conjunction with the VGPM method in consistently capturing ecosystem responses to physical alterations resulting from human activities. Ecologically, this strong correlation underscores the central role of phytoplankton as primary producers in the marine food chain and as early indicators of changes in water health (Bedford et al., 2018). Therefore, fluctuations in Chl-a, as observed before and after the installation of the sea fence, can serve as a key parameter for monitoring anthropogenic impacts on tropical coastal ecosystems.

While the strong correlation between Chl-a and NPP reinforces the reliability of the remote sensing approach, it is important to acknowledge the limitations associated with the absence of in-situ validation. The estimation of Chl-a using the NDCI may be subject to uncertainties caused by several factors, including high turbidity, suspended sediments, atmospheric correction residuals, and shallow water effects common in estuarine environments. These uncertainties can lead to under- or overestimation of Chl-a concentrations, which, when used as input in the VGPM model, may propagate and influence the derived NPP values. Therefore, although the spatial trends and correlations remain consistent, the absolute accuracy of productivity estimates should be interpreted with caution. Incorporating ground-truth data in future studies would enhance model robustness and strengthen the interpretation of remote sensing-derived productivity assessments.

5. CONCLUSION

The findings of this study indicate that the level of primary productivity in the coastal waters of the Kronjo Sub-district is extremely low, falling below the oligotrophic threshold. This reflects limited water fertility and an imbalance within the local ecosystem. The low average values of NPP, along with the narrowing spatial distribution of chl-a, suggest restricted nutrient supply and disrupted phytoplankton dynamics, which play a key role as primary producers in the marine food web. The installation of these fences appears to impede the natural mixing of water masses, thereby intensifying stagnation and promoting the build-up of nutrients in confined zones-conditions which may give rise to localised eutrophication. This situation is further aggravated by a decline in rainfall, resulting in diminished terrestrial runoff that would otherwise serve as a key source of nutrients.

In light of these findings, it is strongly recommended that all sea fence structures, particularly those located in estuarine areas critical for nutrient exchange, be urgently reviewed and dismantled to restore ecological connectivity and natural hydrodynamic flow. Such interventions are essential for supporting primary productivity and preventing further degradation of estuarine ecosystems. Beyond these site-specific recommendations, this study highlights broader implications for coastal spatial governance in Indonesia.

The results underscore the importance of integrating high-resolution ecological monitoring into the enforcement of spatial regulations, such as the Regional Spatial Plan or RTRW and Coastal and Small Islands Zoning Plan or RZWP3K. Although these planning instruments are formally established, they often lack effective enforcement, allowing unregulated physical structures to persist

in ecologically sensitive zones. Strengthening monitoring systems and enforcement mechanisms is therefore critical to ensuring that future coastal development aligns with ecosystem resilience and long-term sustainability goals.

This study successfully achieved its objective of identifying changes in Chl-a concentrations and primary productivity before and after the construction of sea fences and assessing the impact on ecosystem balance. The integration of high-resolution satellite imagery, the NDCI, and the VGPM has proven to effectively detect ecological changes spatially and temporally. It holds potential as a long-term monitoring tool for other tropical coastal regions. Nonetheless, the study was constrained by the absence of in-situ validation data. Future study should incorporate synchronous field-based measurements to enhance the accuracy and robustness of remote sensing-based primary productivity assessments in coastal environments.

ACKNOWLEDGEMENTS

We would like to express our sincere gratitude to the The Freedom to Learn – Independent Campus Program (MBKM), the National Research and Innovation Agency or BRIN, and the Marine Information System Study Program, Indonesia University of Education or UPI. Their support and collaboration have been invaluable in the successful completion of this study. The authors also to thank Planet Labs PBC for providing the high-resolution PlanetScope imagery under a student license through the Planet Education and Research Program.

REFERENCES

Abdullah, A. L., & Dusuki, M. S. A. (2018). Coastal reclamation influence on biological status of coastal waters in Northern Straits of Malacca. *International Journal of Latest Research in Science and Technology, 7*(6), 16-19. doi:10.29111/ijlrst-2018-10959

An Ru., Liu, Y., Qu, C., Zhang, Y., & Wang, Y. (2013). Estimation of chlorophyll-a concentration of case II waters from hyperspectral remote sensing data in NDCI method. *Journal of Lake Sciences, 25*(3), 437-444. (in Chinese with English abstract). doi:10.18307/2013.0319

Ar-ridhaty Akita, E., Gaol, J. L., & Amri, K. (2023). Model Maximum Entropy Untuk Prediksi Daerah Penangkapan Ikan Pelagis Kecil Di Laut Jawa. *Jurnal Ilmu dan Teknologi Kelautan Tropis, 14*(3), 449-461. https://doi.org/10.29244/jitkt.v14i3.45164

Bedford, J., Johns, D. G., Greenstreet, S. P. R., & McQuatters-Gollop, A. (2018). Plankton as prevailing conditions: A surveillance role for plankton indicators within the Marine Strategy Framework Directive. *Marine Policy*. https://doi.org/10.1016/j.marpol.2017.12.021

Behrenfeld, M. J., & Falkowski, P. G. (1997). A consumer's guide to phytoplankton primary productivity models. *Limnology and Oceanography*, *42*(7), 1479-1491. https://doi.org/10.4319/lo.1997.42.7.1479

Dewi, N. N., Kamal, M., Wardiatno, Y., & Rozi. (2018). The exploration of trophic structure modeling using mass balance Ecopath model of Tangerang coastal waters. *IOP Conference Series: Earth and Environmental Science, 137*(1). https://doi.org/10.1088/1755-1315/137/1/012044

Fadlillah, L. N., Sunarto, Widyastuti, M., & Marfai, M. A. (2018). The impact of human activities in the Wulan Delta Estuary, Indonesia. *IOP Conference Series: Earth and Environmental Science, 148*(1). https://doi.org/10.1088/1755-1315/148/1/012032

Fan, W., Xu, Z., Dong, Q., Chen, W., & Cai, Y. (2023). Remote sensing-based spatiotemporal variation and driving factor assessment of chlorophyll-a concentrations in China's Pearl River Estuary. *Frontiers in Marine Science*, *10*, 122. https://doi.org/10.3389/fmars.2023.1226234

Fathia, D. (2021) Analisis produktivitas primer berdasarkan pengukuran kelimpahan fitoplankton dan konsentrasi klorofil-a di perairan Pulau Tangkil, Lampung. Undergraduate thesis. Jurusan Ilmu Kelautan, Fakultas Matematika dan Ilmu Pengetahuan Alam, Universitas Sriwijaya. [Online] Available from: http://repository.unsri.ac.id/ [Accessed: 20 May 2025].

Fitra, F., Zakaria, I. J., & Syamsuardi. (2013). Produktivitas primer fitoplankton di Teluk Bungus. *Biologika, 2*(1), 59-66.

Herdianti, T. P., Yulius., Agus, S. B., Arifin, T., Putra, A., Prihantono, J., Heriati, A., Hartati, S. T., Akhwady, R., Suryono, D. D., Rahmania, R., Ramdhan, M., Hilmawan, A., Ningsih, A., Sadad, S., Mudjijono, M., & Asyiri, A. (2025). Habitat assessment of whale sharks (Rhincodon typus) in Saleh Bay, Indonesia: Linking chlorophyll-a and sea surface temperature using Aqua MODIS data. *Geographia Technica, 20*(2), 52-64. https://doi.org/10.21163/GT_2025.202.04

Jamal, F. (2019). Peran Pemerintah Daerah Dalam Pengelolaan Wilayah Pesisir. Rechtsregel: *Jurnal Ilmu Hukum, 2*(1). https://doi.org/10.32493/rjih.v2i1.2981

Kuang, C., Wang, D., Wang, G., Liu, J., Han, X., & Li, Y. (2024). Impact of reclamation projects on water quality in Jinmeng Bay, China. *Estuarine, Coastal and Shelf Science*. https://doi.org/10.1016/j.ecss.2024.108719

Kumar, R., Kumar, V., Meena, R. C., Meena, P. D., & Kumar, A. (2023). Knowledge mining for the differentiation pattern with respect to the productivity and trophic status of some selected lakes of Western Himalayas. *Frontiers in Environmental Science*, 11, 1009942. https://doi.org/10.3389/fenvs.2023.1009942

Laksana, I. W. (2011) *Analisis pengelolaan wilayah pesisir di Kecamatan Kronjo Kabupaten Tangerang*. Undergraduate thesis. Fakultas Ilmu Sosial dan Ilmu Politik, Universitas Sultan Ageng Tirtayasa. [Online] Available from: http://repositori.untirta.ac.id/ [Accessed: 18th April 2025].

Manuel, A., & Blanco, A. C. (2023). Transformation of the Normalized Difference Chlorophyll Index To Retrieve Chlorophyll-a Concentrations in Manila Bay. International Archives of the Photogrammetry, *Remote Sensing and Spatial Information Sciences*, 217-221. https://doi.org/10.5194/isprs-archives-XLVIII-4-W6-2022-217-2023

Marpaung, S., Prayogo, T., Yati, E., Dwi Purwanto, A., Nandika, M. R., Dirgahayu Domiri, D., & Kushardono, D. (2022). Analisis Karakteristik Net Primary Productivity Dan Klorofil-a Di Laut Banda dan Sekitarnya. *Jurnal Ilmu dan Teknologi Kelautan Tropis, 14*(1), 31-46. https://doi.org/10.29244/jitkt.v14i1.36757

McFeeters, S. K. (1996). The use of the Normalized Difference Water Index (NDWI) in the delineation of open water features. *International Journal of Remote Sensing, 17*(7), 1425-1432. https://doi.org/10.1080/01431169608948714

Mishra, D. R., Schaeffer, B. A., & Keith, D. (2014). Performance evaluation of normalized difference chlorophyll index in northern Gulf of Mexico estuaries using the Hyperspectral Imager for the Coastal Ocean. *GIScience and Remote Sensing, 51*(2), 175-198. https://doi.org/10.1080/15481603.2014.895581

Mishra, S., & Mishra, D. R. (2012). Normalized difference chlorophyll index: A novel model for remote estimation of chlorophyll-a concentration in turbid productive waters. *Remote Sensing of Environment, 117*, 394-406. https://doi.org/10.1016/j.rse.2011.10.016

Nugraheni, D. D., Zainuri, M., & Afi Ati, R. N. (2014). Studi Tentang Variabilitas Klorofil-a dan Net Primary Productivity di Perairan Morosari, Kecamatan Sayung, Demak. *Journal of Oceanography, 3*(4), 519 – 527. Retrieved from: https://ejournal3.undip.ac.id/index.php/joce/article/view/6905

Nuzapril, M., Susilo, S. B., & Panjaitan, J. P. (2017). Hubungan antara konsentrasi klorofil-a dengan tingkat produktivitas primer menggunakan citra satelit Landsat-8. *Jurnal Teknologi Perikanan dan Kelautan*, 8(1), 105-114. https://doi.org/10.24319/jtpk.8.105-114

Nuzapril, M., Susilo, S. B., & Panjaitan, J. P. (2019). Sebaran produktivitas primer kaitannya dengan kondisi kualitas air di perairan Karimun Jawa. *Jurnal Segara, 15*(1), 9-17. https://doi.org/10.15578/segara.v15i1.7559

Pearson, K. (1896). VII. Mathematical contributions to the theory of evolution.—III. Regression, heredity, and panmixia. *Philosophical Transactions of the Royal Society of London. Series A, containing papers of a mathematical or physical character*, (187), 253-318.

Prabuwono, A. S., Kunarso, K., Wirasatriya, A., & Antoni, S. (2023). Investigation of chlorophyll-a variability in Red Sea using satellite-based meteorology and oceanography data. *Geographia Technica, 18*(2), 238-248. https://doi.org/10.21163/GT_2023.182.18

Sambah, A. B., Oktavia, T. D., Kusuma, D. W., Iranawati, F., Hidayati, N., & Wijaya, A. (2020). Oceanographic variability and its influence on pelagic fish catch in the Bali Strait. *Berkala Penelitian Hayati, 26*(1), 8-16. https://doi.org/10.23869/bphjbr.26.1.20202

Saulquin, B., Gohin, F., & Fanton d'Andon, O. (2019). Interpolated fields of satellite-derived multi algorithm chlorophyll-a estimates at global and European scales in the frame of the European Copernicus-Marine Environment Monitoring Service. *Journal of Operational Oceanography, 12*(1), 47-57. https://doi.org/10.1080/1755876X.2018.1552358

Suardiani, N. K., Arthana, I. W., & Kartika, G. R. A. (2018). Produktivitas Primer Fitoplankton pada Daerah Penangkapan Ikan di Taman Wisata Alam Danau Buyan, Buleleng, Bali. *Current Trends in Aquatic Science, 1*(1), 8. https://doi.org/10.24843/ctas.2018.v01.i01.p02

Walpole, R. E., Myers, R. H., Myers, S. L. & Ye, K. E. (2011). *Probability and Statistics for Engineers and Scientists. 9th ed. [Online] Boston, Pearson Education*. Available from: https://spada.uns.ac.id/pluginfile.php/221008/mod_resource/content/1/ProbabilityStatistics_for_Engineers Scientists(9th_Edition)_Walpole.pdf [Accessed 16th June 2025].

Wasehun, E. T., Beni, L. H., Di Vittorio, C. A., Zarzar, C. M., & Young, K. R. L. (2025). Comparative analysis of Sentinel-2 and PlanetScope imagery for chlorophyll-a prediction using machine learning models. *Ecological Informatics, 85*, 102988. https://doi.org/10.1016/j.ecoinf.2024.102988

Werdell, P. J., Franz, B. A., Bailey, S. W., Feldman, G. C., Boss, E., Brando, V. E., Dowell, M., Hirata, T., Lavender, S. J., Lee, Z., Loisel, H., Maritorena, S., Mélin, F., Moore, T. S., Smyth, T. J., Antoine, D., Devred, E., Fanton d'Andon, O. H., & Mangin, A. (2013). Generalized ocean color inversion model for retrieving marine inherent optical properties. *Applied Optics, 52*(10), 2019-2037. https://doi.org/10.1364/AO.52.002019

Wijayanti, T. I., Mitasari, W., Nday, S. U., & Subandrio, A. (2022). Valuasi Lingkungan Melalui Contingent Valuation Methode (CVM) dalam Revitalisasi Waduk Rowo Jombor Klaten. *Jurnal Pembangunan Wilayah Dan Kota, 18*(3), 283-295. https://doi.org/10.14710/pwk.v18i3.36930

Yanuar., Ibnusina, F., Hutahaean, A. A., Doktoralina, C. M., Caniago, A., Alisafira, S., Rumingkang, N. S., Sa'badini, S. A., Mangkurat, R. S. B., Kholil, & Prasetyo, T. (2023). *Menuju Puncak Pengintegrasian Rencana Tata Ruang Darat dan Laut*. 1-90.

Yulius., Aidina, V., Ramdhan, M., & Daulat, A. (2021). Fishing Ground Mapping Based on Chlorophyll-A Distribution Using Aqua Modis Satellite Imagery in The Fisheries Management Area (FMA) 712. *E3S Web of Conferences, 324*, 10-12. https://doi.org/10.1051/e3sconf/202132401007